

Published in final edited form as:

Bioorg Med Chem. 2015 February 1; 23(3): 602–611. doi:10.1016/j.bmc.2014.11.043.

IND2, a pyrimido[1'',2'':1,5]pyrazolo[3,4-b]quinoline derivative, circumvents multi-drug resistance and causes apoptosis in colon cancer cells

Chandrabose Karthikeyan¹, Crystal Lee², Joshua Moore², Roopali Mittal³, Esther A. Suswam⁴, Kodye L Abbott⁵, Satyanarayana R. Pondugula⁵, Upender Manne⁴, Narayanan K. Narayanan⁶, Piyush Trivedi^{*,1}, and Amit K. Tiwari^{*,2}

¹School of Pharmaceutical Sciences, Rajiv Gandhi Proudyogiki Vishwavidyalaya, Bhopal, MP, India 462033

²Department of Biomedical Sciences, College of Veterinary Medicine, Nursing and Allied Health, Tuskegee University, Tuskegee, AL 36088, USA

³Pediatric Gastroenterology and Nutrition, Oklahoma State University, Oklahoma City, OK, 73104

⁴Department of Pathology and Comprehensive Cancer Center, University of Alabama at Birmingham, Birmingham, AL 35294, USA

⁵Department of Anatomy, Physiology and Pharmacology, College of Veterinary Medicine, Auburn University, Auburn, AL 36849

⁶New York University School of Medicine, New York, NY.

Abstract

Naturally occurring condensed quinolines have anticancer properties. In efforts to find active analogues, we designed and synthesized eight polycyclic heterocycles with a pyrimido[1'',2'':1,5]pyrazolo[3,4-b]quinoline framework (**IND** series). The compounds were evaluated for activity against colon (HCT-116 and S1-MI-80), prostate (PC3 and DU-145), breast (MCF-7 and MDAMB-231), ovarian (ov2008 and A2780), and hepatocellular (HepG2) cancer cells and against non-cancerous Madin Darby canine kidney (MDCK), mouse embryonic fibroblast (NIH/3T3), and human embryonic kidney cells (HEK293). **IND-2**, a 4-chloro-2-methyl pyrimido[1'',2'':1,5]pyrazolo[3,4-b]quinoline, exhibited more than tenfold selectivity and potent cytotoxic activity against colon cancer cells relative to the other cancer and non-cancer cells. With five additional colon cancer cell lines (HT-29, HCT-15, LS-180, LS-174, and LoVo), **IND-2** had similar

© 2014 Elsevier Ltd. All rights reserved.

*Corresponding Authors: **Amit K. Tiwari**, PhD Assistant Professor, Pharmacology, Department of Biomedical Sciences, CVMNAH, Tuskegee University, Tuskegee, AL 36088 Ph: 334-714-4644 atiwari@mytu.tuskegee.edu **Dr. Piyush Trivedi** Professor, School of Pharmaceutical Sciences, Rajiv Gandhi Proudyogiki Vishwavidyalaya, Bhopal, MP, India 462033. Ph: +91755 2678883 piyush.trivedi@rgtu.net.

Publisher's Disclaimer: This is a PDF file of an unedited manuscript that has been accepted for publication. As a service to our customers we are providing this early version of the manuscript. The manuscript will undergo copyediting, typesetting, and review of the resulting proof before it is published in its final citable form. Please note that during the production process errors may be discovered which could affect the content, and all legal disclaimers that apply to the journal pertain.

Conflict of Interest: Authors declare no conflict of interest.

cytotoxicity and selectivity, and submicromolar concentrations caused changes in the morphology of HCT-116 and HCT-15 cells. **IND-2** did not activate the transactivating function of the pregnane X receptor (PXR), indicating that it does not induce PXR-regulated ABCB1 or ABCG2 transporters. Indeed, **IND-2** was not a substrate of ABCB1 or ABCG2, and it induced cytotoxicity in HEK293 cells overexpressing ABCB1 or ABCG2 to the same extent as in normal HEK293 cells. **IND-2** was cytotoxic to resistant colon carcinoma S1-MI-80 cells, approximately three- and fivefold more than SN-38 and topotecan, respectively. In HCT-116 colon cancer cells, **IND-2** produced concentration-dependent changes in mitochondrial membrane potential, leading to apoptosis, and sub-micromolar concentrations caused chromosomal DNA fragmentation. These findings suggest that, by increasing apoptosis, **IND-2** has potential therapeutic efficacy for colorectal cancer.

1. Introduction

Despite progress made in cancer research, particularly in early detection and treatment, cancer continues to be a leading cause of death worldwide. In the US alone, 585,720 cancer deaths are projected to occur in 2014 [1]. Recent advances in the molecular biology of cancer have led to development of new anticancer agents. However, most treatments are inadequately effective due to toxicity and to development of drug resistance [2]. Therefore, discovery of chemotherapeutic agents with reduced toxicity and with the capacity to circumvent drug resistance is a challenging task for medicinal chemists.

Due to their natural abundance and broad spectrum of antitumor activity, nitrogen heterocyclic compounds containing condensed quinoline ring systems (**Figure 1A**) are important biological and medicinal scaffolds for anticancer drug discovery [3]. These compounds consist of a planar polycyclic pharmacophore, generally a tetracyclic ring system, along with one or two flexible substituent groups that allow for DNA intercalation and/or inhibition of DNA re-ligation by topoisomerases [4]. For instance, camptothecin (**Figure 1A**), a naturally occurring indolizinoquinoline, elicits potent antitumor activity through selective inhibition of topoisomerase I [5]. Two water-soluble derivatives of camptothecin, topotecan and irinotecan (**Figure 1A**), have received FDA approval for the treatment of ovarian, cervical, lung, and colon cancer [6]. Other examples of naturally occurring, condensed quinoline systems with antitumor activity are cryptoleptine [7, 8], neocryptoleptine [8], and luotonin A [9] (**Figure 1A**).

The clinical efficacy of naturally occurring, condensed quinolines has led to efforts for the design, synthesis, and development of anticancer agents based on this scaffold. Many such efforts have involved condensing the quinoline ring with various heterocycles such as indole, bezimidazole, or a pyrimidone (**Figure 1B**). For example, a quinoline ring condensed with an indole moiety led to indoloquinolines (**Figure 1B**), structurally analogous to cryptoleptine, which showed both DNA intercalation and topoisomerase inhibition [10, 11]. Substituted 9-anilinothiazolo[5,4-b]quinolines (**Figure 1B**), which incorporate a quinoline scaffold fused with a thiazole ring, demonstrated cytotoxicity against four cancer cell lines [cervical (HeLa), colorectal (SW480 and SW620), and chronic myelogenous leukemia (K-562)] and also inhibited human topoisomerase II [12].

Annulation of the benzimidazole ring to the quinoline moiety resulted in cyclic benzimidazole[1,2-a]quinolines (**Figure 1B**) with antiproliferative effects on various cancer cells [13]. Some pyrimido[4',5':4,5]thieno(2,3-b)quinoline-4(3H)-ones (**Figure 1B**), with structural analogy to ellipticine, showed potent anti-leukemic activity *in vitro* and *in vivo* [14].

Despite its structural similarity to many of the aforementioned anticancer molecules, (ellipticine, cryptolepine), the pyrimido[1'',2'':1,5]pyrazolo[3,4-b]quinoline framework (**Figure 1B**) is one of the least studied classes of tetracyclic condensed quinolines. The presence of a planar polycyclic pharmacophore and its amenability to structural manipulation makes this scaffold an ideal template for medicinal chemistry efforts targeting cancer. Prompted by these findings and in continuation of our research on novel polycyclic heterocycles with antitumor activity, we extended our interest to the pyrimido[1'',2'':1,5]pyrazolo[3,4-b]quinoline system and synthesized a series of eight 2-methyl pyrimido[1'',2'':1,5]pyrazolo[3,4-b]quinoline derivatives (**IND series**), and evaluated their activity against various cancer cells. The rationale for the choice of these eight compounds for synthesis and anticancer activity evaluation is owing to their structural analogy with ellipticine and cryptolepine and also based on the literature reports which suggest attachment of hydroxyl [15], chloro [16] or dialkyl amino group either directly or through a flexible alkyl amino side chain [17][18] to polycyclic heteroaromatic ring contributes to cytotoxic activity of ellipticine and cryptolepine.

The present report is the first on the synthesis and anticancer activity of pyrimido[1'',2'':1,5]pyrazolo[3,4-b]quinolines. This work led to the discovery of 4-chloro-2-methylpyrimido[1'',2'':1,5]pyrazolo[3,4-b]quinoline (**IND-2**), which has potent cytotoxic and apoptosis-inducing properties in colon cancer cells.

2. Results and Discussion

2.1. Chemistry

The synthetic protocol followed to obtain 2-methylpyrimido[1'',2'':1,5]pyrazolo[3,4-b]quinoline and its amino alkyl derivatives is depicted in **Figure 2A**. The synthesis of starting material, 2-chloroquinoline-3-carbaldehyde (**1**), was accomplished from suitable acetanilides *via* the Vilsmeier-Haack reaction, following a previously described procedure [19]. 2-Chloroquinoline-3-carbaldehyde, on treatment with hydroxylamine hydrochloride in aqueous ammonia in presence of ceric ammonium nitrate, furnished 2-chloroquinoline-3-carbonitrile (**2**) [20], which, on reaction with hydrazine hydrate under reflux conditions, afforded 1H-pyrazolo[3,4-b]quinolin-3-amine (**3**) [21]. 1H-Pyrazolo[3,4-b]quinolin-3-amine, refluxed in ethanol with ethyl acetoacetate, underwent a cyclo-condensation reaction to give 2-methylpyrimido[1'',2'':1,5]pyrazolo[3,4-b]quinoline-4(1H)-one (**IND-1**) [22]. This was further halogenated with phosphorous oxychloride to give the key intermediate, 4-chloro, 2-methyl pyrimido[1'',2'':1,5]pyrazolo[3,4-b]quinoline (**IND-2**), which, on reaction with appropriate alkyl amines in ethanol, gave the corresponding amino-alkyl substituted 2-methylpyrimido[1'',2'':1,5]pyrazolo[3,4-b]quinoline derivatives (**IND-3 to IND-8**). **Figure 2B** shows the structures proposed for **IND-1 to IND-8**, consistent with IR, mass spectral, and ¹H-NMR spectral data.

2.2. Biological Evaluation

2.2.1. Growth curves, cell cytotoxicity, and morphological analysis for IND-1 and IND-2 and their amino alkyl derivatives (IND-3 to IND-8)—IND-1 and IND-2 and their amino alkyl derivatives (IND-3 to IND-8) were evaluated for cytotoxic effects on nine types of cancer cells, i.e., colon (HCT-116 and S1), prostate (PC3 and DU-145), breast (MCF-7 and MDAMB-231), ovarian (ov2008 and A2780), and hepatocellular carcinoma (HepG2) and on three non-cancerous cells, including canine kidney (MDCK), mouse embryonic fibroblast (NIH/3T3), and human embryonic kidney (HEK293) cell lines. The 3-(4,5-dimethylthiazol-2-yl)-2,5-diphenyltetrazolium bromide (MTT) assay was used. All compounds were tested at concentrations ranging from 0.1 μM to 100 μM . The 50% minimum inhibitory concentrations (IC_{50}) are summarized in **Table 1**.

IND-1 and IND-2 and their amino alkyl derivatives (IND-3 to IND-8) exhibited variable degrees of growth inhibitory activity towards the nine human cancer cell lines and three non-cancerous cell lines (Table 1). The lead compound, IND-1, showed only a modest inhibitory activity ($\text{IC}_{50} > 40 \mu\text{M}$) on the tested cells. Other compounds, with the exception of IND-2, showed moderately more or less cytotoxic activity relative to IND-1. Of the pyrimido [1'',2'':1,5]pyrazolo[3,4-b]quinolines with an amino alkyl side chain (IND-3 to IND-8), IND-3, with a 4-(2-aminoethyl)diethylamine substitution, was most effective against ovarian (ov2008, A2780) and breast (MDAMB-231) cancer cells, with IC_{50} values ranging between 44-50 μM . A similar cytotoxic profile against colon cancer (HCT-116 and S1) and MDCK cells was observed for IND-6, which has a 4-(2-aminoethyl)diethylamine substitution. Among the eight compounds studied, IND-2, with a chloro substitution on the fourth position of the pyrimido[1,2:1,5]-pyrazolo[3,4-b]quinoline ring, showed selective and potent growth inhibition against colon cancer cells. The IC_{50} values of IND-2 against HCT-116 and S1 cells were 0.6 μM and 0.8 μM , respectively. Prostate cancer cells (PC-3 and DU-145) were also inhibited by IND-2, with an IC_{50} values ranging from 0.8 μM to 1.2 μM . Further, IND-2 showed moderate growth inhibitory activity ($\text{IC}_{50} > 10 \mu\text{M}$) against breast (MCF-7 and MDAMB-231) cancer cells. Overall, these results established that the 4-chloro substitution is significant to the anticancer activity of 2-methylpyrimido[1'',2'':1,5]pyrazolo[3,4-b]quinolines and that compound IND-2 was a promising candidate for further studies with colon cancer cells.

2.2.2. IND-2 exhibits selective and potent cytotoxic activity on various colon cancer cells—The effects of compound IND-2 on colon carcinoma cells prompted us to expand our studies to other types of colon cancer cells (HCT-15, HT-29, Lovo, LS-180, and LS-174). All these were sensitive to IND-2 at concentrations ranging from ~0.6 to 1.0 μM (Table 2, Figure 3A and 3B). Notably, IND-2 was 10-15 fold more selective for inhibition of colon cancer cells relative to HEK293 cells (Figure 3A and 3B); 10-30 fold more selective for other cancer cells (breast, ovarian, and hepatocellular carcinoma) (Table 1); and 20-40 fold more selective relative to NIH/3T3 mouse fibroblast cells and MDCK cells (Table 1). After 68 hrs of treatment of HCT-116, HCT-15, and HEK293 cells with 0, 0.5, 2, or 10 μM IND-2, morphological changes, complementing the cytotoxicity data, were evident in all the cells (Figure 3C shows representative images). In sum, the cytotoxic effect of

IND-2 on colon cancer cells is particularly notable because of its selectivity and its IC_{50} values of $< 1 \mu M$.

2.2.3. IND-2 does not activate pregnane X receptor (PXR), is not a substrate of ABCB1 or ABCG2 transporters, and is cytotoxic to chemoresistant colon cancer cells—PXR is a ligand-dependent nuclear receptor involved in regulating the expression of ATP-binding cassette (ABC) transporters, including ABCB1 (a.k.a. P-glycoprotein) and ABCG2 (a.k.a. breast cancer resistance protein, BCRP) [23, 24]. Activation of PXR by xenobiotics leads to chemoresistance [24], a concern in drug development and clinical therapy. The possible activation of PXR by **IND-2** was examined with HepG2 cell-based reporter gene assays. Although rifampicin (RIF), an agonist of human PXR, induced PXR transactivation of CYP3A4 promoter activity, **IND-2** at 1 or 10 μM did not affect PXR transactivation (**Figure 4A**), showing that **IND-2** does not activate PXR at concentrations cytotoxic to colon cancer cells and indicating that **IND-2** does not induce PXR-mediated drug resistance in cancer cells. Similar to RIF, **IND-2** at 10 μM was marginally cytotoxic, although **IND-2** at 1 μM was non-cytotoxic (**Figure 4B**), showing that the lack of effect of **IND-2** on PXR was not due to cytotoxicity.

Multi-drug resistance (MDR) factors, such as ABCB1 and ABCG2 transporters, present limitations for the development of anticancer agents [2]. These transporters are expressed in a variety of solid and hematological malignancies, where they are involved in the efflux of various therapeutic drugs, leading to MDR [25]. Ideally, drugs that are not substrates for these transporters are preferred as anticancer agents. **IND-2** was screened against ABCB1- and ABCG2-overexpressing cells, and its effects were compared with positive controls paclitaxel and mitoxantrone, respectively. There was no substantial resistance to **IND-2** in ABCB1- or ABCG2-overexpressing cells, as all the cells were sensitive at similar concentrations of **IND-2** (**Figure 4C**), indicating that **IND-2** is not a substrate for ABCB1 and ABCG2 transporters. These results support our PXR analysis (**Figure 4A**).

Additionally, the cytotoxic potential of **IND-2** was evaluated for a G482 mutant ABCG2-overexpressing, drug-resistant colon cancer cell line, S1-M1-80. S1-M1-80 cells showed significant resistance ($p < 0.001$) to SN-38, an active metabolite of irinotecan and topotecan (**Figure 4D**). **IND-2**, however, inhibited the resistant S1-M1-80 cells 3-5 fold more potently ($P < 0.001$) than SN-38 and topotecan (**Figure 4D**). This could be because: **a**) **IND-2** did not interact with ABCG2 transporters, was not effluxed by resistant S1-M1-80 cells, and maintained its cytotoxic concentration, or **b**) **IND-2** blocked the ABCG2 transporters and **IND-2** retained its cytotoxic potential in resistant S1-M1-80 cells. If the second reason is true, may be beneficial in combination chemotherapy against colorectal and other tumors with agents that are substrates of ABCG2 transporters. However, further mechanistic experiments including ATPase, photo-affinity labeling assays, and combination chemotherapy are necessary to confirm the interactions of **IND-2** with ABCB1 and ABCG2 transporters.

2.2.4. IND-2 induces reduces mitochondrial membrane potential and causes apoptosis and DNA fragmentation in colon cancer cells—Inappropriately regulated apoptosis is implicated in cancer. Whereas, mitochondrial dysfunction is involved

in signaling processes that initiate apoptotic events, loss of membrane asymmetry, cytochrome c, and other apoptogenic factors released from mitochondria initiate apoptotic cell death. In the process of apoptosis, phosphatidylserine (PS), otherwise located on the cytoplasmic surface, is translocated from the inner to the outer leaflet of the plasma membrane. The extracellular exposed PS has high affinity for binding to the human vascular anticoagulant, annexin V, a 35–36 kDa, Ca²⁺-dependent, phospholipid-binding protein. This principle is used to determine the binding of annexin V, labeled with a fluorophore or biotin, to exposed PS on the outer leaflet and thereby to identify apoptotic cells [26].

Live cells, 63.11% of untreated HCT-116 cells with intact mitochondrial membranes, are seen in quadrant I of **Figure 5A**. Of these cells, 27.56% had a loss in mitochondrial membrane potential and had started the process of apoptosis. Treatment with **IND-2**, even at 1 μM, for 4 hr produced a significant loss ($p < 0.01$) of membrane potential in 68.46% of the cells, as seen in quadrant II of **Figure 5A**. At 10 μM, **IND-2** treatment for 4 hr showed that almost all the cells (98.36%) had no or low mitochondrial membrane potential and thus were primed to undergo apoptosis (quadrant II of **Figure 5A**). These data show that **IND-2** produces concentration-dependent decreases in mitochondrial potential of HCT-116 colon cancer cells, leading to apoptosis.

The extent of **IND-2**-induced DNA damage in HCT-116 colon cancer cells was assessed by chromosomal DNA fragmentation. Treatment with 2.5 μM **IND-2** for 6 hr led to fragmentation of chromosomal DNA (**Figure 5B**). In contrast, chromosomal DNA of untreated cells was intact. These results indicate that **IND-2** induces DNA breakage at multiple positions across chromosomal DNA, leading to apoptosis.

Summary: In summary, this work has led to the discovery of a lead 4-chloro-2-methyl pyrimido[1'',2'':1,5]pyrazolo[3,4-b]quinoline (**IND-2**) with potent cytotoxic and apoptosis-inducing properties for colon cancer cells, without being an activator of PXR or a substrate for ABCB1 or ABCG2 transporters. Further mechanistic studies, including gene microarray analyses, are being performed to elucidate the effects of **IND-2** on colon cancer cells at the genomic level. Further studies are underway in our laboratory to examine whether structural modification at the benzo ring of quinoline moiety can result in more potent analogues of **IND-2** with potential therapeutic applications in colon cancer and the results of the study will be communicated in due course. Pharmacokinetic-pharmacodynamic experiments, including colon cancer xenografts will be conducted with animals to establish the selectivity and cytotoxicity of most potent **IND-2** like molecule for therapy of colorectal cancer.

4. Experimental section

4.1. Chemistry

All commercial chemicals and solvents were reagent grade and were used without further treatment, unless otherwise noted. Melting points were determined in open glass capillaries on a Veego digital melting point apparatus and were uncorrected. The infrared (IR) spectra were recorded on a Shimadzu FT-IR 8400S IR spectrophotometer with an ATR accessory. ¹H-NMR spectra were recorded on a Bruker Avance II 400 spectrometer with chloroform-*d* or dimethyl sulfoxide (DMSO)-*d*₆ as solvent and trimethylsilane as an internal

standard. Mass spectral analyses were accomplished with an Applied Biosystem Qtrap 3200 MS/MS system in ESI mode. Elemental analyses were performed with a Vario Micro cube CHNS analyzer (Elementar, NJ, USA). Reactions were monitored by thin-layer chromatography on pre-coated silica gel aluminum plates (Kieselgel 60, 254, E. Merck, Germany); zones were detected visually under ultraviolet irradiation.

4.2. Synthesis of 2-methylpyrimido[1'',2'':1,5]pyrazolo[3,4-b]quinoline derivatives (IND-1 to IND-8)

4.2.1. 2-Chloroquinoline-3-carbaldehyde (1)—Dimethyl formamide (9.6 mL, 0.125 mol) was cooled to 0°C in a flask equipped with a drying tube, and phosphoryl chloride (32.2 mL, 0.35 mol) was added dropwise with stirring. To this solution, acetanilide (0.05 mol) was added, and, after 5 min, the solution was heated under reflux at 75 °C for 16.5 hr in a temperature-controlled oil bath. After completion of the reaction, as indicated by TLC, the solution was cooled to room temperature and poured into 100 mL of ice water. The precipitate was collected by filtration and recrystallized from ethyl acetate to yield 2-chloroquinoline-3-carbaldehyde as pale yellow crystals. 64 % yield. M.P. 148-150°C (Lit. 149°C) [19]; FT-IR (ATR) ν (cm⁻¹): 3044 (aromatic C-H), 2870 (aldehyde C-H), 1684(C=O), 1574(C=N), 760(C-Cl); ¹H-NMR (400 MHz, chloroform-*d*) δ 10.57 (s, 1H), 8.77 (s, 1H), 8.08 (d, *J* = 8.5 Hz, 1H), 7.99 (d, *J* = 8.1 Hz, 1H), 7.90 (t, *J* = 7.7 Hz, 1H), 7.66 (t, *J* = 8.0 Hz, 1H); MS-API: [M+H]⁺ 192 (calculated 191.01).

4.2.2. 2-chloroquinoline-3-carbonitrile (2)—A suspension of 2-chloroquinoline-3-carbaldehyde (0.01 mol) in 30% aqueous ammonia (30 mL) was stirred for 5 min at room temperature, resulting in formation of a turbid solution. To this, ceric ammonium nitrate (0.01 mol) was added with constant stirring at 0°C. After completion of the reaction (monitored by TLC, 10-15 min), the mixture was extracted with chloroform-ethyl acetate (5:3), dried with anhydrous sodium sulfate, and concentrated under reduced pressure to give a crude product, which was crystallized in ethanol to give pure 2-chloroquinoline-3-carbonitrile as pale yellow crystals. Yield: 82 %. M.P. 162°-163°C (Lit. 162°C) [20]; FT-IR (ATR) ν (cm⁻¹): 3059 (aromatic (C-H), 2232 (C N), 1580 (C=N), 750 (CCl); ¹H NMR (400 MHz, chloroform-*d*) δ 8.63 – 8.51 (m, 1H), 8.07 (dd, *J* = 8.4, 1.1 Hz, 1H), 7.98 – 7.83 (m, 2H), 7.69 (ddd, *J* = 8.2, 6.9, 1.2 Hz, 1H); MS-API: [M+H]⁺ 189 (calculated 188.01).

4.2.3. 1H-Pyrazolo[3,4-b]quinolin-3-amine (3)—2-Chloroquinoline-3-carbonitrile 2 (1.88 g, 0.01 mol) was refluxed with hydrazine hydrate (25 mL) for 5 hr. The reaction mixture was cooled, poured into water, and the resulting precipitate was filtered off and crystallized from ethanol to give reddish orange crystals. Yield: 76%. M.P. >275°C (Lit. >300°C) [21]; FT-IR (ATR) ν (cm⁻¹): 3377, 3298, 3179 (NH, NH₂); 3049 (aromatic C-H), 1616 (C=N); ¹H-NMR (DMSO-*d*₆, 400 MHz): δ [27] 11.71 (s, 1H), 8.72 (s, 1H), 7.97 (d, *J*=8.3 Hz, 1H), 7.82 (d, *J*=8.5 Hz, 1H), 7.66 (t, *J*=7.6 Hz, 1H), 7.34 (t, *J*=7.4 Hz, 1H), 5.89 (s, 2H); MS-API: [M+H]⁺ 185 (calculated 184.07).

4.2.4. 2-Methylpyrimido[1'',2'':1,5]pyrazolo[3,4-b]quinoline-4(1H)-one (IND-1)—A mixture of 1H-pyrazolo[3,4-b]quinolin-3-amine (1.1 g, 0.006 mol), ethyl acetoacetate (0.75 mL, 0.006 mol), and glacial acetic acid (15 mL) was refluxed for 5 hr. The solid

product that formed after cooling was collected and recrystallized from dioxane as wine red crystals of **4**. Yield: 69%. M.P. > 275°C; FT-IR (ATR) ν (cm⁻¹): 3180 (NH), 3061 (aromatic C-H), 2845 (aliphatic C-H) 1693 (C=O), 1516(C=C); ¹H NMR (400 MHz, DMSO-*d*₆) δ 11.90 (s, 1H), 9.33 (s, 1H), 8.15 (d, *J* = 7.9 Hz, 1H), 7.87 (t, *J* = 7.6 Hz, 1H), 7.74 (d, *J* = 8.5 Hz, 1H), 7.44 (t, *J* = 7.4 Hz, 1H), 6.25 (s, 1H), 2.37 (s, 3H); MS-API (M+H)⁺251.0 (calculated 250.09). Calculated for C₁₄H₁₀N₄O; C, 67.19; H, 4.03; N, 22.39; Found: C, 67.23; H, 3.98; N, 22.42.

4.2.5. 4-Chloro-2-methyl pyrimido[1",2":1,5]pyrazolo[3,4-b]quinoline (IND-2)—

A solution of phosphorus oxychloride (10 mL, 0.107 mol) and **4** (1.25 g, 0.005 mol) was heated under reflux for 1 hr. The reaction mixture was brought to room temperature, excess reagent was removed *in vacuo*, and the residue was triturated with ice water. The chlorinated product was extracted with dichloromethane. The organic layer was separated, dried over anhydrous sodium sulfate, and filtered. The filtrate was concentrated and purified by column chromatography (silica gel with ethyl acetate: petroleum ether, 2:3) to afford **5**. Yield: 52%. M.P. = 165-167°C; FT-IR (ATR) ν (cm⁻¹): 3057, 3011 (aromatic C-H), 2849 (aliphatic C-H), 1618, 1587 (C=C, C=N), 754 (C-Cl); ¹H NMR (400 MHz, DMSO-*d*₆) δ 9.55 (s, 1H), 8.22 (d, *J* = 8.5 Hz, 1H), 8.09 (s, 1H), 8.03 (d, *J* = 8.7 Hz, 1H), 7.82 (t, *J* = 7.6 Hz, 1H), 7.46 (t, *J* = 7.2 Hz, 1H), 2.77 (s, 3H); MS-API (M+H)⁺269.0 (calculated 268.05). Calculated for C₁₄H₉ClN₄; C, 62.52; H, 3.38; N, 20.92. Found: C, 62.64; H, 3.47; N, 21.01.

4.2.6. General procedure for synthesis of 4-amino alkyl 2-methylpyrimido[1,2 : 1,5]-pyrazolo[3,4-b]quinolines (IND-3 to IND-8)—Various alkyl amines (1.2 mmol) and **5** (1 mmol) in absolute ethanol (5 mL) were refluxed for 2-6 hr. The ethanol was removed by evaporation, and the crude products were purified by crystallization in a mixture of ethyl acetate: petroleum ether (6:4).

4.2.6.1. N,N,2-Trimethyl benzopyrido[2',3':3,4]pyrazolo[1,5-a]pyrimidin-4-amine (IND-3):

Yield: 69%. M.P. 203-205°C; FT-IR (ATR) ν (cm⁻¹):3047 (aromatic C-H), 2849 (aliphatic C-H), 1633, 1597 (C=C, C=N); ¹H-NMR (400 MHz, DMSO-*d*₆) δ 9.30 (s, 1H), 8.09 (d, *J* = 8.2 Hz, 1H), 7.88 (d, *J* = 8.7 Hz, 1H), 7.71 (t, *J* = 7.2 Hz, 1H), 7.32 (t, *J* = 7.4 Hz, 1H), 6.90 (s, 1H), 3.46 (s, 6H), 2.62 (s, 3H); MS-API (M+H)⁺278.0 (Calculated 277.13). Calculated for C₁₆H₁₅N₅; C, 69.29; H, 5.45; N, 25.25. Found: C, 69.32; H, 5.44; N, 25.26.

4.2.6.2. 2-Methyl-4-(morpholin-4-yl)benzopyrido[2',3':3,4]pyrazolo[1,5a]pyrimidine (IND-4):

Yield: 65%. M.P. 264-267°C; FT-IR (ATR) ν (cm⁻¹): 3015 (aromatic C-H), 2900, 2860 (aliphatic C-H), 1628, 1587 (C=C, C=N), 1111(C-O-C); ¹H-NMR (400 MHz, DMSO-*d*₆) δ 9.89 (s, 1H), 8.37 (d, *J* = 8.2 Hz, 1H), 8.16 – 7.96 (m, 2H), 7.64 (t, *J* = 7.3 Hz, 1H), 7.42 (s, 1H), 4.02 (t, *J* = 4.6 Hz, 4H), 3.85 (t, *J* = 4.6 Hz, 4H), 2.68 (s, 3H). MS-API (M +H)⁺320.2 (calculated 319.14). Calculated for C₁₈H₁₇N₅O; C, 67.70; H, 5.37; N, 21.93; Found: C, 67.68; H, 5.38; N, 21.92.

4.2.6.3. N,N-dimethyl-N'-(2-methylbenzopyrido[2',3':3,4]pyrazolo[1,5-a]pyrimidin-4-yl)ethane-1,2-diamine (IND-5): Yield: 73%. M.P. 237-239°C; FT-IR (ATR) ν (cm⁻¹):

3173 (NH), 2814 (Aliphatic C-H) 1636, 1582(C=C, C=N). ¹H-NMR (400 MHz, DMSO-*d*₆) δ [27] 9.29 (s, 1H), 8.69 (t, *J*=5.6 Hz, 1H), 8.08 (d, *J*=8.3 Hz, 1H), 7.88 (d, *J*=8.8 Hz, 1H), 7.69 (t, *J*=7.6 Hz, 1H), 7.31 (t, *J*=7.5 Hz, 1H), 6.87 (s, 1H), 3.65 (t, *J*=4.4 Hz, 4H), 2.61 (s, 3H), 2.28 (s, 6H); MS-API (M+H)⁺321.2 (Calculated 320.17). Calculated for C₁₈H₂₀N₆; C, 67.48; H, 6.29; N, 26.23; Found: C, 67.47; H, 6.30; N, 26.22.

4.2.6.4. N,N-diethyl-N'-(2-methylbenzopyrido[2',3':3,4]pyrazolo[1,5-a]pyrimidin-4-yl)ethane-1,2-diamine (IND-6): Yield 76%. M.P. 178-181°C; FT-IR (ATR) ν (cm⁻¹): 3192 (NH), 2803 (aliphatic C-H) 1633, 1576 (C=C, C=N); ¹H-NMR (400 MHz, chloroform-*d*) δ [27] 9.12 (s, 1H), 8.10 (d, *J*=8.8 Hz, 1H), 7.97 (d, *J*=8.3 Hz, 1H), 7.74 (t, *J*=7.7 Hz, 1H), 7.36 (t, *J*=7.4 Hz, 1H), 6.60 (s, 1H), 3.91 (s, 2H), 3.49 (s, 2H), 3.08 (d, *J* = 8.6 Hz, 4H), 2.42 (s, 3H), 1.32 (t, *J* = 7.2 Hz, 6H); MS-API (M+H)⁺349.2 (Calculated 348.21). Calculated for C₂₀H₂₄N₆; C, 68.94; H, 6.94; N, 24.12; Found: C, 68.89; H, 6.92; N, 24.18.

4.2.6.5. N,N-dimethyl-N'-(2-methylbenzopyrido[2',3':3,4]pyrazolo[1,5-a]pyrimidin-4-yl)propane-1,3-diamine (IND-7): Yield: 77%. M.P. 200-202°C; FT-IR (ATR) ν (cm⁻¹): 3237 (NH), 3047 (aromatic C-H) 2851, 2785 (aliphatic C-H) 1636, 1604 (C=C, C=N); ¹H-NMR (DMSO-*d*₆, 400 MHz): δ [27] 9.28 (s, 1H), 8.55 (t, *J*=5.5 Hz, 1H), 8.08 (d, *J*=8.3 Hz, 1H), 7.88 (d, *J*=8.8 Hz, 1H), 7.69 (t, *J*=7.5 Hz, 1H), 7.31 (t, *J*=7.3 Hz, 1H), 6.87 (s, 1H), 3.51 - 3.56 (m, 2H), 2.61 (s, 3H), 2.33 (t, *J*=6.5 Hz, 2H), 2.16 (s, 6H), 1.82 (t, *J*=6.8 Hz, 2H); MS-API (M+H)⁺335.2 (calculated 334.19). Calculated for C₁₉H₂₂N₆; C, 68.24; H, 6.63; N, 25.13; Found: C, 67.98; H, 6.72; N, 25.08.

4.2.6.6. N,N-diethyl-N'-(2-methylbenzopyrido[2',3':3,4]pyrazolo[1,5-a]pyrimidin-4-yl)propane-1,3-diamine (IND-8): Yield: 81%. M.P. 184-186°C; FT-IR (ATR) ν (cm⁻¹): 3154 (NH), 3046 (aromatic C-H), 2920, 2810 (aliphatic C-H) 1635, 1580 (C=C, C=N); ¹H NMR (DMSO-*d*₆, 400MHz): δ [27] 9.28 (s, 1H), 8.68 (br. s., 1H), 8.08 (d, *J*=8.3 Hz, 1H), 7.88 (d, *J*=8.8 Hz, 1H), 7.69 (t, *J*=7.6 Hz, 1H), 7.31 (t, *J*=7.4 Hz, 1H), 6.83 (s, 1H), 3.53 (q, *J*=6.0 Hz, 2H), 2.61 (s, 3H), 2.41 - 2.50 (m, 6H), 1.81 (quin, *J*=6.5 Hz, 2H), 0.97 (t, *J*=7.1 Hz, 6H); MS-API (M+H)⁺363.2 (calculated 362.22). Calculated for C₂₁H₂₆N₆; C, 69.58; H, 7.23; N, 23.19; Found: C, 69.46; H, 7.12; N, 23.31.

4.3. Biology

DMEM media, 0.25% trypsin, propidium iodide, paclitaxel, buffers, and reagents were purchased from VWR (VWR International Inc., Suwanee, GA). MitoTracker Red and Alexa Fluor 488 annexin V kits for flow cytometry were purchased from Life Sciences (Molecular Probes Inc., Invitrogen, Eugene, OR). DMSO and RIF were purchased from Sigma (St. Louis, MO). pcDNA3-hPXR and pGL3-CYP3A4-luc plasmids were as previously described [23, 28].

4.3.1. Cell culture—Colon carcinoma cell lines, HCT-116, HCT-15, HT-29, Lovo, LS-180, LS-174, S1 (a clone of LS174T cells), and S1-M1-80 (resistant); and prostatic cancer cell lines, DU-145 and PC-3; breast carcinoma cells, MDA-MB-231 and MCF-7; ovarian cancer cells, ov2008 and A2780; canine kidney MDCK cells; mouse fibroblast NIH/3T3 cells; human liver cells HepG2; human embryonic kidney cells, HEK293/

pcDNA3.1 (control, non-cancerous cells transfected with empty vector); HEK293/ABCB1 (a P-glycoprotein overexpressing cell line); and HEK293/R2 (ABCG2-overexpressing cells) were grown as adherent monolayers in flasks with Dulbecco's Modified Eagle Medium (DMEM) supplemented with 10% fetal bovine serum (FBS) in a humidified incubator containing 5% CO₂ at 37°C. A G482 mutant ABCG2-overexpressing, drug-resistant colon cancer cell line, S1-M1-80, was maintained in medium with 80 μM mitoxantrone [29]. The assay media for PXR transactivation assays included phenol red-free DMEM (Lonza) supplemented with 5% charcoal/dextran-treated FBS (HyClone) and the other additives. MDR cell lines HEK293/R2, HEK293/ABCB1, and S1-M1-80 were obtained from Dr. Gary Kruh at the University of Chicago, Illinois.

4.3.2. PXR transactivation assay—HepG2 cells were transfected with pcDNA3-hPXR and CYP3A4-luc plasmids using FuGENE 6 (Promega). After 24 hr of transfection in growth media, 10,000 cells were plated into wells of 96-well culture plates (PerkinElmer), and treated with DMSO, RIF, or **IND-2** for an additional 24 hr. At 48 hr after transfection, a luciferase assay was performed to measure luminescence using the Neolite Reporter Gene Assay System (PerkinElmer) and a FLUOstar Optima microplate reader (BMG Labtech). Normalized CYP3A4 promoter activity was expressed as fold induction over the DMSO control. Cell viability was measured in parallel by CellTiter-Glo luminescent assays (Promega), which determine the number of metabolically active cells by quantifying the ATP present. Luminescence was measured with a FLUOstar Optima plate reader (BMG Labtech).

4. 3.3. Cell cytotoxicity as determined by MTT assays and morphological analysis—The MTT assay [30] was used to determine cytotoxicity of the compounds to the following cells: HCT-116, HCT-15, HT-29, LS-180, LS-174, Lovo, S1, DU-145, PC-3, MDA-MB-231, MCF-7, MDCK, mouse fibroblast NIH/3T3, human primary embryonic kidney HEK293/pcDNA3.1 (control, non-cancerous, transfected with empty vector), HEK293/R2, and HEK293/ABCB1. Briefly, the cells were harvested with trypsin and suspended at a final concentration of 5×10^3 cells/well (HCT-116, HCT-15, HT-29, DU-145, PC-3, HEK293/pcDNA3.1, HEK293/R2 and HEK293/ABCB1) or 6×10^3 cells/well (MCF-7, MDCK, NIH/3T3, LS-180, LS-174, Lovo, S1, and MDA-MB-231). Cells were seeded (180 μL/well) into 96-well multiplates. Different concentrations of pyrimido[1,2:1,5]-pyrazolo[3,4-b]quinolines (20 μL/well) were added. After 72 hr of incubation, 20 μL of MTT solution (4 mg/mL) was added to each well, and the plates were incubated for a further 4 hr, allowing viable cells to convert the yellow-colored MTT into dark-blue formazan crystals. Subsequently, the medium was discarded, and 100 μL of DMSO was added into each well to dissolve the formazan crystals. The absorbance was determined at 570 nm with an OPSYS microplate Reader (DYNEX Technologies, Inc., Chantilly, VA, USA). The means \pm SD concentrations were calculated from at least three experiments performed in triplicate. The IC₅₀ values were calculated from survival curves using the Bliss method.

At 68 hr, cells, with or without treatment, were photographed by use of an inverted microscope (Olympus, BX53F) with fluorescent lamps and digital cameras. The data were acquired and analyzed by CellSens software.

4.3.4. Mitochondrial membrane potential and DNA fragmentation analysis—

Mitochondrial membrane potential and apoptosis were measured for colon cancer HCT-116 cells using MitoTracker Red and Alexa Fluor 488 annexin V kits for flow cytometry (Molecular Probes Inc., Invitrogen, Eugene, OR). Briefly, apoptosis was induced by exposing HCT-116 cells (seeded in 6 well-plates) with or without **IND-2** at 1 or 10 μM concentrations for 4 hr. Equal amounts of cells were harvested, and, to each mL of cells, 4 μL of 10 μM MitoTracker Red working solution was added. Cells were stained for 30 min at 37 °C in an atmosphere of 5% CO_2 . The cells were washed with PBS and suspended in 100 μL of 1X annexin-binding buffer, to which 5 μL of Alexa Fluor 488 annexin V was added. Cells were incubated for an additional 15 min, after which 400 μL of 1X annexin-binding buffer was added. The stained cells were counted by flow cytometry, measuring the fluorescence emission at 530 nm and 585 nm (BD FACSCalibur Flow Cytometer using FlowJo FACS data analysis software).

A characteristic feature of apoptosis is induction of oligonucleosomal DNA fragmentation by cytotoxic compounds, which activate nucleases that degrade the higher-order chromatin structure of DNA into mono- and oligonucleosomal DNA fragments [31]. To establish the mode of action of **IND-2** in colon cancer cytotoxicity, a DNA fragmentation assay was performed. Apoptotic degradation of DNA was analyzed by agarose gel electrophoresis. Briefly, HCT-116 cells were cultured in the presence or absence of **IND-2** (2.5 μM) for 6 hr. Genomic DNA was extracted from the cells by use of Promega Wizard Genomic DNA purification kits (Promega Corporation, Madison, WI) and resolved on 1% agarose gels at 40 V for 4 hr. DNA was visualized by ethidium bromide staining and photographed.

4. 3.4. Statistics—Unless otherwise indicated, all experiments were repeated at least three times, and differences were determined by Student's t-test (GraphPad Prism version 5.04). Results were presented as means \pm standard deviations (SD). Statistical significance was determined at $P < 0.05$.

Acknowledgements

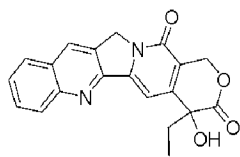
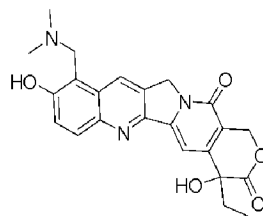
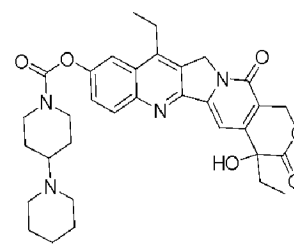
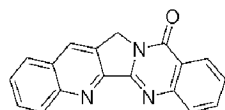
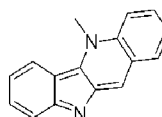
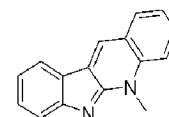
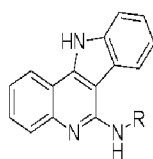
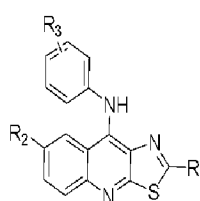
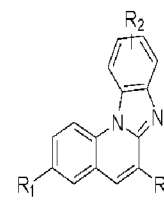
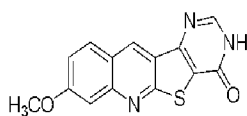
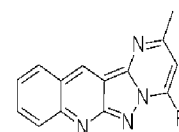
We thank Dr. Donald Hill (UAB) for editorial assistance. We would like to thank Mr. Jason White (Tuskegee University) and Patrick Flannery (Auburn University) for technical assistance; Tuskegee RCMI Core grant number (G12MD007585-23); IBS-REU program to support summer research student Joshua Moore; MSM/TU/UAB Comprehensive Cancer Center Partnership [NCI] (U54 CA118623 (TU) and U54 CA118948 (UAB)) to Drs. Tiwari, Suswam and Manne; Auburn University Research Initiative in Cancer and Animal Health and Disease Research Grants to Dr. Pondugula. We are also thankful to the Council of Scientific and Industrial Research (CSIR), New Delhi, India for a Senior Research Fellowship (C. Karthikeyan). We would also like to thank Dr. Tao at Auburn University for sharing the FLUOstar Optima plate reader.

References

1. Siegel R, Ma J, Zou Z, Jemal A. Cancer statistics, 2014. CA: a cancer journal for clinicians. 2014; 64:9–29. [PubMed: 24399786]

2. Gottesman MM. Mechanisms of cancer drug resistance. *Annual review of medicine*. 2002; 53:615–627.
3. Lavrado J, Moreira R, Paulo A. Indoloquinolines as scaffolds for drug discovery. *Current medicinal chemistry*. 2010; 17:2348–2370. [PubMed: 20491639]
4. Manpadi M, Uglinskii PY, Rastogi SK, Cotter KM, Wong Y-SC, Anderson LA, Ortega AJ, Van slambrouck S, Steelant WFA, Rogelj S, Tongwa P, Antipin MY, Magedov IV, Kornienko A. Three-component synthesis and anticancer evaluation of polycyclic indenopyridines lead to the discovery of a novel indenoheterocycle with potent apoptosis inducing properties. *Organic & Biomolecular Chemistry*. 2007; 5:3865–3872. [PubMed: 18004468]
5. Liu LF, Desai SD, Li TK, Mao Y, Sun M, Sim SP. Mechanism of action of camptothecin. *Annals of the New York Academy of Sciences*. 2000; 922:1–10. [PubMed: 11193884]
6. Garcia-Carbonero R, Supko JG. Current Perspectives on the Clinical Experience, Pharmacology, and Continued Development of the Camptothecins. *Clinical Cancer Research*. 2002; 8:641–661. [PubMed: 11895891]
7. Ansah C, Mensah KB. A review of the anticancer potential of the antimalarial herbal cryptolepis sanguinolenta and its major alkaloid cryptolepine. *Ghana medical journal*. 2013; 47:137–147. [PubMed: 24391229]
8. Dassonneville L, Lansiaux A, Wattelet A, Wattez N, Mahieu C, Van Miert S, Pieters L, Bailly C. Cytotoxicity and cell cycle effects of the plant alkaloids cryptolepine and neocryptolepine: relation to drug-induced apoptosis. *European journal of pharmacology*. 2000; 409:9–18. [PubMed: 11099695]
9. Cagir A, Jones SH, Gao R, Eisenhauer BM, Hecht SM, Luotonin A. A Naturally Occurring Human DNA Topoisomerase I Poison. *Journal of the American Chemical Society*. 2003; 125:13628–13629. [PubMed: 14599178]
10. Lu C-M, Chen Y-L, Chen H-L, Chen C-A, Lu P-J, Yang C-N, Tzeng C-C. Synthesis and antiproliferative evaluation of certain indolo[3,2-c]quinoline derivatives. *Bioorganic & Medicinal Chemistry*. 2010; 18:1948–1957. [PubMed: 20171108]
11. Godlewska J, Badowska-Rosłonek K, Ramza J, Kaczmarek Ł, Peczy ska-Czoch W, Opolski A. New saccharide derivatives of indolo [2, 3-b] quinoline as cytotoxic compounds and topoisomerase II inhibitors. *Radiology and Oncology*. 2004; 38
12. Loza-Mejía MA, Olvera-Vázquez S, Maldonado-Hernández K, Guadarrama-Salgado T, González-Sánchez I, Rodríguez-Hernández F, Solano JD, Rodríguez-Sotres R, Lira-Rocha A. Synthesis, cytotoxic activity, DNA topoisomerase-II inhibition, molecular modeling and structure–activity relationship of 9-anilinothiazolo [5, 4-*c*] quinoline derivatives. *Bioorganic & medicinal chemistry*. 2009; 17:3266–3277. [PubMed: 19364657]
13. Perin N, Uzelac L, Piantanida I, Karminski-Zamola G, Kralj M, Hranjec M. Novel biologically active nitro and amino substituted benzimidazo [1, 2-*c*] quinolines. *Bioorganic & medicinal chemistry*. 2011; 19:6329–6339. [PubMed: 21964184]
14. Sharma S, Panjamurthy K, Choudhary B, Srivastava M, Shahabuddin M, Giri R, Advirao GM, Raghavan SC. A novel DNA intercalator, 8-methoxy pyrimido [4', 5': 4, 5] thieno (2, 3-b) quinoline-4 (3H)-one induces apoptosis in cancer cells, inhibits the tumor progression and enhances lifespan in mice with tumor. *Molecular carcinogenesis*. 2013; 52:413–425. [PubMed: 22213363]
15. Harding MM, Grummitt AR. 9-hydroxyellipticine and derivatives as chemotherapy agents. *Mini reviews in medicinal chemistry*. 2003; 3:67–76. [PubMed: 12570841]
16. Arguello F, Alexander MA, Greene JF Jr, Stinson SF, Jordan JL, Smith EM, Kalavar NT, Alvord WG, Klabansky RL, Sausville EA. Preclinical evaluation of 9-chloro-2-methylellipticinium acetate alone and in combination with conventional anticancer drugs for the treatment of human brain tumor xenografts. *Journal of cancer research and clinical oncology*. 1998; 124:19–26. [PubMed: 9498830]
17. Larue L, Rivalle C, Muzard G, Paoletti C, Bisagni E, Paoletti J. A new series of ellipticine derivatives (1-(alkylamino)-9-methoxyellipticine). Synthesis, DNA binding, and biological properties. *Journal of medicinal chemistry*. 1988; 31:1951–1956. [PubMed: 3172128]

18. Lavrado J, Paulo A, Gut J, Rosenthal PJ, Moreira R. Cryptolepine analogues containing basic aminoalkyl side-chains at C-11: Synthesis, antiplasmodial activity, and cytotoxicity. *Bioorganic & Medicinal Chemistry Letters*. 2008; 18:1378–1381. [PubMed: 18207399]
19. Meth-Cohn O, Narine B, Tarnowski B. A versatile new synthesis of quinolines and related fused pyridines, Part 5. The synthesis of 2-chloroquinoline-3-carbaldehydes. *Journal of the Chemical Society, Perkin Transactions*. 1981; 1:1520–1530.
20. Srivastava A, Singh R. Vilsmeier-Haack reagent: A facile synthesis of 2-chloro-3-formylquinolines from N-arylacetamides and transformation into different functionalities. *Indian Journal of Chemistry Section B*. 2005; 44:1868.
21. El-Sayed OA, Aboul-Enein HY. Synthesis and Antimicrobial Activity of Novel Pyrazolo[3,4-b]quinoline Derivatives. *Archiv der Pharmazie*. 2001; 334:117–120. [PubMed: 11382146]
22. Bakhite EA-G. Synthesis of New Pyrazolo[3,4-b]quinolines, Thieno[2,3-b]quinolines and Related Condensed Heterocyclic Systems. *Journal of the Chinese Chemical Society*. 2001; 48:1175–1183.
23. Pondugula SR, Dong H, Chen T. Phosphorylation and protein-protein interactions in PXR-mediated CYP3A repression. *Expert opinion on drug metabolism & toxicology*. 2009; 5:861–873. [PubMed: 19505191]
24. Pondugula SR, Mani S. Pregnane xenobiotic receptor in cancer pathogenesis and therapeutic response. *Cancer letters*. 2013; 328:1–9. [PubMed: 22939994]
25. Tiwari AK, Sodani K, Dai CL, Ashby CR Jr, Chen ZS. Revisiting the ABCs of multidrug resistance in cancer chemotherapy. *Current pharmaceutical biotechnology*. 2011; 12:570–594. [PubMed: 21118094]
26. Koopman G, Reutelingsperger CP, Kuijten GA, Keehnen RM, Pals ST, van Oers MH. Annexin V for flow cytometric detection of phosphatidylserine expression on B cells undergoing apoptosis. *Blood*. 1994; 84:1415–1420. [PubMed: 8068938]
27. Leonessa F, Green D, Licht T, Wright A, Wingate-Legette K, Lippman J, Gottesman MM, Clarke R. MDA435/LCC6 and MDA435/LCC6MDR1: ascites models of human breast cancer. *Br J Cancer*. 1996; 73:154–161. [PubMed: 8546900]
28. Pondugula SR, Tong AA, Wu J, Cui J, Chen T. Protein phosphatase 2C β regulates human pregnane X receptor-mediated CYP3A4 gene expression in HepG2 liver carcinoma cells. *Drug Metab Dispos*. 2010; 38:1411–1416. [PubMed: 20538721]
29. Robey RW, Medina-Perez WY, Nishiyama K, Lahusen T, Miyake K, Litman T, Senderowicz AM, Ross DD, Bates SE. Overexpression of the ATP-binding cassette half-transporter, ABCG2 (Mxr/BCrp/ABCP1), in flavopiridol-resistant human breast cancer cells. *Clin Cancer Res*. 2001; 7:145–152. [PubMed: 11205902]
30. Carmichael J, DeGraff WG, Gazdar AF, Minna JD, Mitchell JB. Evaluation of a tetrazolium-based semiautomated colorimetric assay: assessment of chemosensitivity testing. *Cancer Res*. 1987; 47:936–942. [PubMed: 3802100]
31. Henkels KM, Turchi JJ. Cisplatin-induced Apoptosis Proceeds by Caspase-3-dependent and -independent Pathways in Cisplatin-resistant and -sensitive Human Ovarian Cancer Cell Lines. *Cancer Research*. 1999; 59:3077–3083. [PubMed: 10397248]
32. Wu CP, Woodcock H, Hladky SB, Barrand MA. cGMP (guanosine 3',5'-cyclic monophosphate) transport across human erythrocyte membranes. *Biochem Pharmacol*. 2005; 69:1257–1262. [PubMed: 15794947]

A.**Camptothecin****Topotecan****Irinotecan****Luotonin A****Cryptolepine****Neocryptolepine****B.****Indolo[3,2-c]quinoline derivatives****Thiazolo[5,4-b]quinoline derivatives****Benzimidazo[1,2-a]quinoline derivatives****8-methoxy pyrimido [4', 5': 4, 5] thieno (2, 3-b) quinoline-4 (3H)-one****2-Methylpyrimido[1'',2'':1,5]pyrazolo[3,4-b]quinoline derivatives****Figure 1.**

(A) Natural product-derived, condensed quinoline-ring systems with anticancer activity. (B) Synthetically derived, condensed quinoline ring systems with anticancer activity.

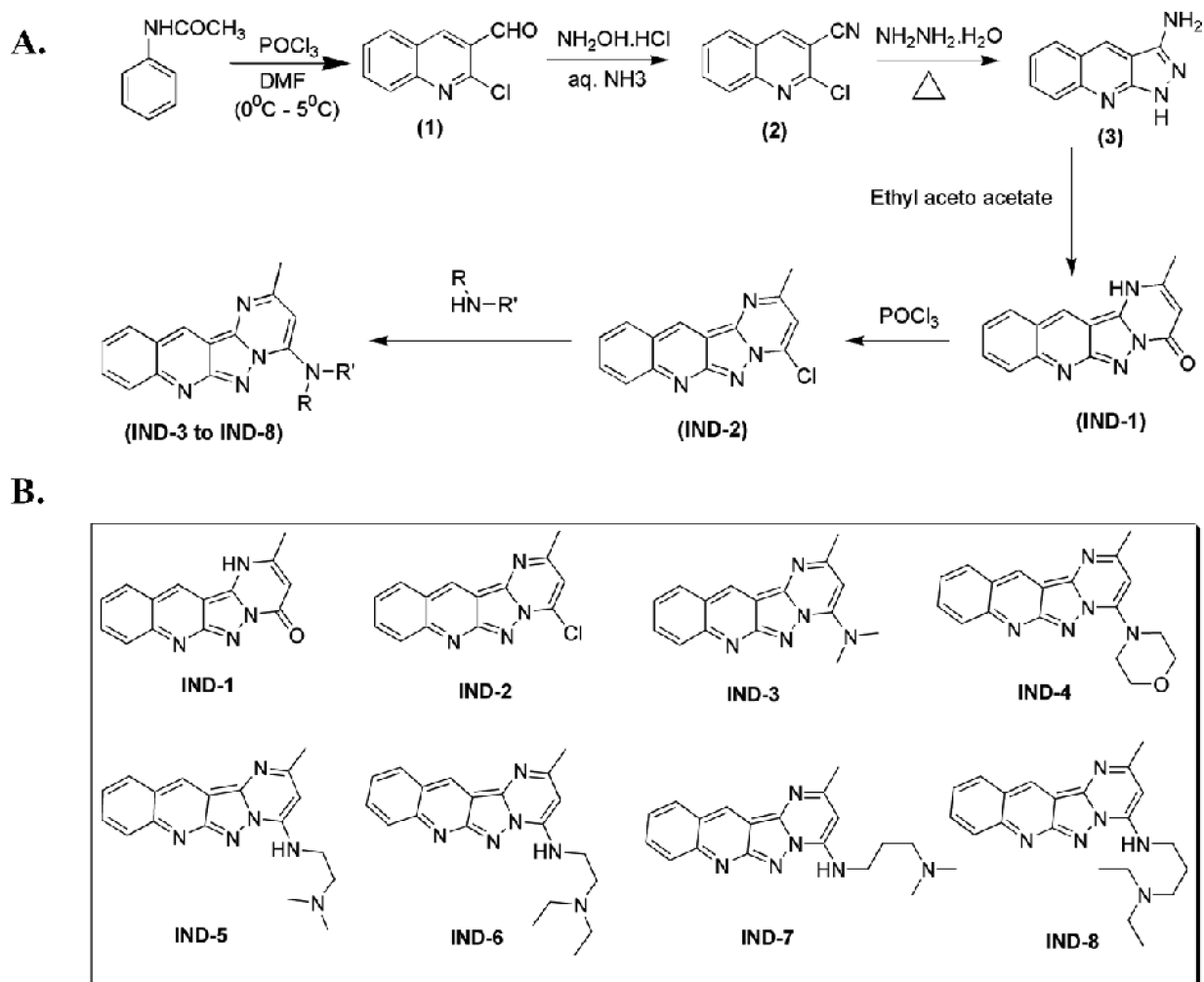


Figure 2.
(A) Synthetic scheme for alkyl amino-substituted, 2-methylpyrimido[1'',2'':1,5]pyrazolo[3,4-b]quinoline derivatives. **(B)** Synthetically derived **IND series** analogues with a 2-methylpyrimido[1'',2'':1,5]pyrazolo[3,4-b]quinoline ring.

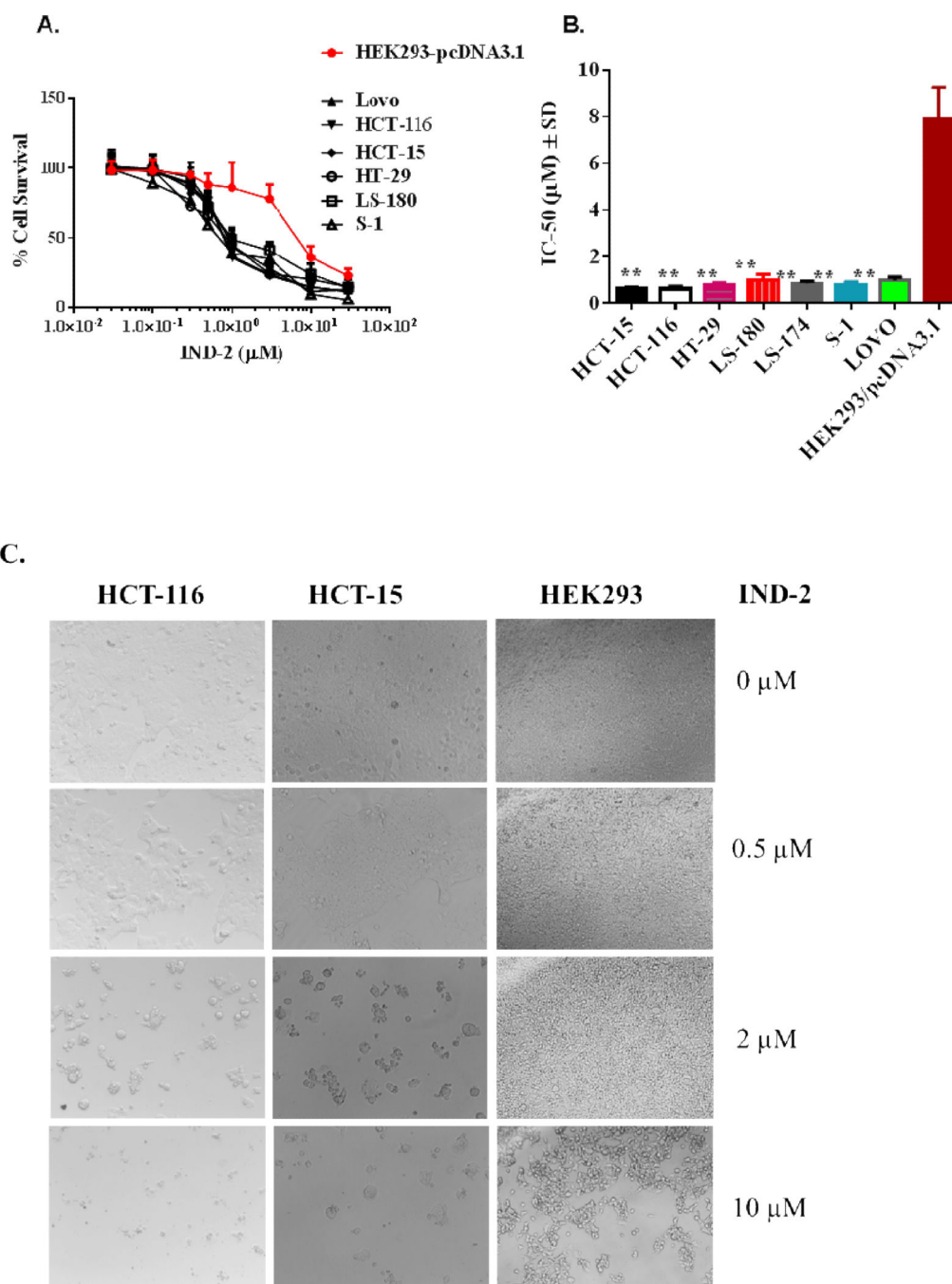


Figure 3. Cytotoxic effects of **IND-2** are shown as (A) survival of colon cancer cells S1, HCT-116, HCT-15, HT-29, Lovo, and LS-180 compared to that of human embryonic kidney cells, HEK293/pcDNA3.1, and (B) IC_{50} values of **IND-2** for colon cancer cells S1, HCT-116, HCT-15, HT-29, Lovo, and LS-180 relative to human embryonic kidney cells (HEK293/pcDNA3.1). Cell survival was determined by the MTT assay. IC_{50} values are represented as means \pm SD of three independent experiments performed in triplicate. Statistically, *, $P < 0.05$; **, $P < 0.01$, colon cancer cells versus the HEK293/pcDNA3.1. (C) Morphological

analysis of the cytotoxic effects of IND-2 (0, 0.5, 2 and 10 [μ M]) on colon cancer cells, HCT-116 and HCT-15; prostate cancer cells, DU-145; and human embryonic kidney cells HEK293, exposed for 68 hr, was made by microscopy at 20X. The cells were photographed for each triplicate treatment with an inverted microscope (Olympus, BX53F) with fluorescent lamps and digital cameras. A representative figure is shown for each treatment. The data were acquired and analyzed with CellSens software.

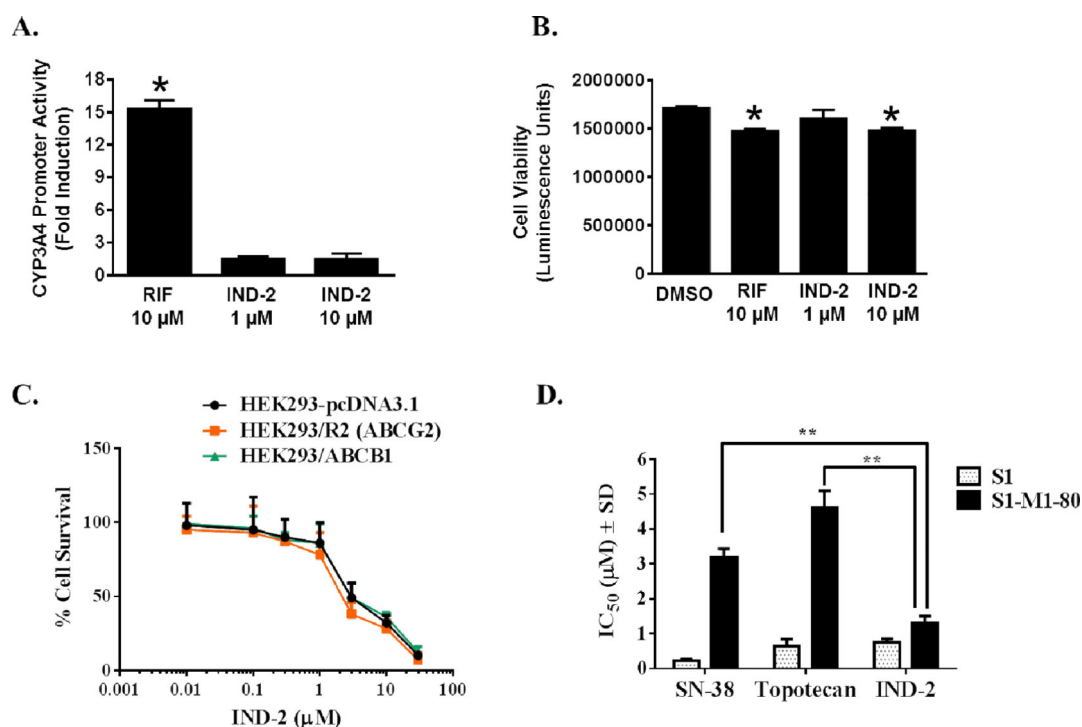


Figure 4. IND-2 does not induce human PXR transactivation of CYP3A4 promoter activity (A) CYP3A4 promoter activity was determined in HepG2 cells after transient cotransfection with pGL3-CYP3A4-luc reporter and pcDNA3-hPXR plasmids for 24 hr, followed by treatment with DMSO, RIF, or **IND-2** for an additional 24 hr. The induction of CYP3A4 promoter activity was normalized as fold increase over the DMSO control. Data represent means \pm SD from three independent experiments. Statistical significance (*, $p < 0.05$) was determined with Student's t test by comparing the effects of RIF or **IND-2** with DMSO. (B) Effect of **IND-2** on HepG2 cell viability. During the PXR transactivation studies, viability of HepG2 cells was determined simultaneously in parallel experiments with the CellTiter-Glo luminescent cell viability assay kit and the data are expressed as luminescence units. Data represent the means \pm SD of triplicate determinations. Statistical significance (*, $p < 0.05$) was determined with Student's t test by comparing the effects of RIF or **IND-2** with DMSO. (C) Effect of **IND-2** on the survival of cells overexpressing ABCB1 or ABCG2. [32] Effects of **IND-2**, topotecan, and SN-38 on S1 and S1-M1-80 cells. MTT cytotoxicity assays were used to measure survival of HEK293/pcDNA3.1, HEK293/R2, HEK293/ABCB1, S1, and S1-M1-80 cells. Data points represent the means \pm SD of triplicate determinations. Representative results from three independent experiments, each performed in triplicate, are shown.

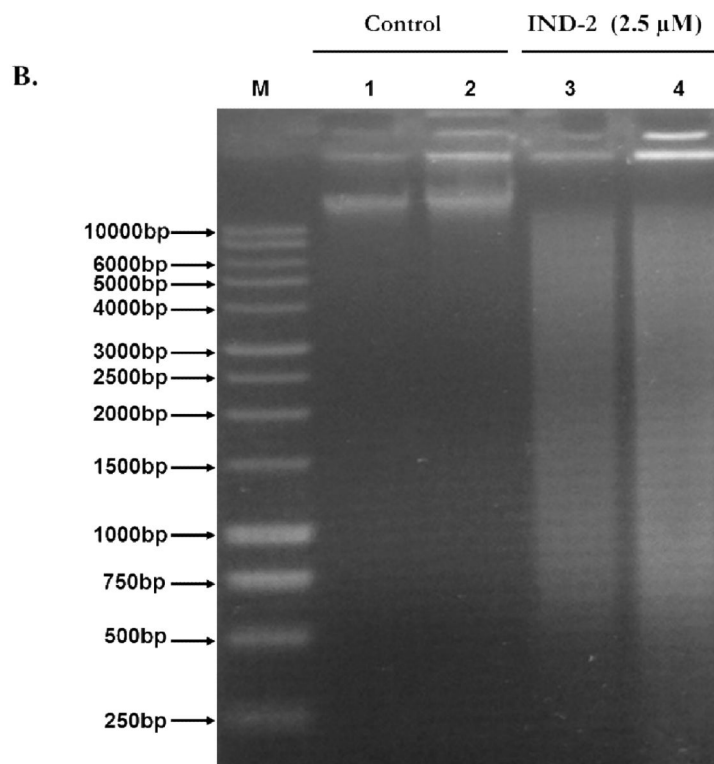
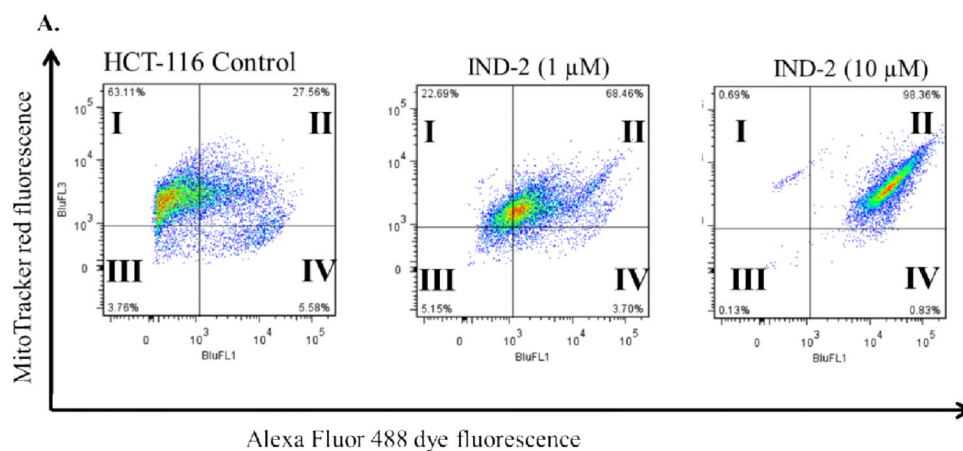


Figure 5. Effects of IND-2 on mitochondrial membrane potential and DNA fragmentation (A). HCT-116 cells in complete medium were exposed to **IND-2** (0, 1, or 10 [proportional] μ M) for 4 hr. Cells were then treated with the reagents of the MitoTracker Red and Alexa Fluor 488 annexin V kits for flow cytometry. Representative results from two independent experiments, each performed in triplicate, are shown. (B) **IND-2** induced DNA damage in HCT-116 cells. Chromosomal DNA was extracted from HCT-116 cells and resolved on a 1% agarose gel at 40 V for 6 hr. Lane 1: 'M', Marker; Lanes 2–3: untreated

HCT cells, 500 ng and 1 μ g, respectively; Lanes 4–5: HCT cells incubated with **IND-2** (2.5 μ M) for 6 hr.

Table 1

Activity of 2-methylpyrimido[1",2":1,5]pyrazolo[3,4-b]quinoline derivatives against various cell lines (cancerous and non-cancerous).

IND series	IC50 ± SD, μM					
	HCT-116	S1	PC3	DU-145	ov2008	A2780
	Colon		Prostate		Ovarian	
IND-1	62.6 ± 12.5	63.6 ± 23.5	46.5 ± 6.9	63.8 ± 7.9	88.6 ± 10.4	74.3 ± 12.4
IND-2	0.6 ± 0.1 **	0.8 ± 0.1 **	0.9 ± 0.2 **	1.2 ± 0.3 **	17.4 ± 2.1	11.6 ± 1.4
IND-3	53.6 ± 11.7	58.3 ± 7.4	88.8 ± 7.1	28.6 ± 11.1	47.9 ± 3.9	49.9 ± 7.2
IND-4	88.9 ± 12.3	67.4 ± 9.5	78.3 ± 4.2	78.6 ± 4.9	±100 ± NA	±100 ± NA
IND-5	65.8 ± 2.6	69.8 ± 3.7	79.8 ± 6.2	59.9 ± 5.7	±100 ± NA	±100 ± NA
IND-6	45.8 ± 5.0	44.6 ± 11.8	62.5 ± 9.7	43 ± 5.4	78.1 ± 15.2	87.5 ± 9.5
IND-7	71.6 ± NA	83.4 ± 7.4	60.5 ± 12.1	67.3 ± 7.4	87.6 ± 5.9	65.8 ± 12.4
IND-8	57.3 ± 15.8	53.7 ± 17.8	78.5 ± 5.2	56.2 ± 19.1	65.3 ± 8.2	55.7 ± 6.4

IND series	NORMAL CELLS					
	HepG2	MCF-7	MDAMB-231	MDCK	NIH/3T3	HEK 293/pcDNA.3.1
	Liver	Breast	Canine kidney	Mouse fibroblast	Embryonic kidney	
IND-1	89.5 ± 12.6	88.7 ± 12.1	76.9 ± 10.1	±100 ± NA	98.4 ± 9.5	69.6 ± 23.8
IND-2	9.7 ± 2.4	7.4 ± 6.2	9.7 ± 5.0	19.7 ± 2.3	23.6 ± 4.2	7.8 ± 1.3
IND-3	67.9 ± 10.4	79.6 ± 12.8	44.8 ± 8.7	89.9 ± 10.4	87.0 ± 12.3	46.1 ± 6.9
IND-4	±100 ± NA	98.4 ± 12.6	88.2 ± 10.5	±100 ± NA	±100 ± NA	67.2 ± 7.9
IND-5	±100 ± NA	70.6 ± 11.7	48.7 ± 16.7	±100 ± NA	±100 ± NA	93.4 ± 9.9
IND-6	67.4 ± 10.5	53.5 ± 6.3	58.8 ± 13.1	41.6 ± 26.6	48.2 ± 20.0	67.4 ± 10.5
IND-7	73.2 ± 7.2	±100 ± NA	76.1 ± 12.6	87.0 ± 22.5	±100 ± NA	39.9 ± 14.5
IND-8	89.9 ± 9.6	67.6 ± 8.8	34.6 ± 13.7	77.5 ± 9.8	±100 ± NA	41.8 ± 5.4

Cell survival assay was determined by the MTT assay. IC₅₀ values are represented as means ± SD of three independent experiments performed in triplicate. A mean IC₅₀ value of 100 μM was the cut off. NA, not assessed.

*P < 0.05

** P < 0.01, versus the control group (Student's t-test).

Table 2IC₅₀ values for IND-2 inhibition of various colon cancer cell lines

Colon cancer cells	IC ₅₀ ± SD ^a , nM
IND-2	
HCT-15	670.6 ± 48.9
HCT-116	634.5 ± 120.1
HT-29	790.8 ± 103.5
LS-180	1023.5 ± 230.6
LS-174	874.6 ± 89.7
S1	798.3 ± 137.4
Lovo	993.8 ± 142.6

Cell survival was determined by the MTT assay. The values represent the means ± SD of at least three independent experiments performed in triplicate.